Received: December 28, 2023. Revised: January 26, 2024.

INASS

International Journal of
Intelligent Engineering & Systems

http://www.inass.org/

Hybridization of Improved Northern Goshawk Optimization and Line Loadability Index for Reconfiguration Considering Solar and Electric Vehicles

Lalitha Kondisetti[1]* **Katragadda Swarnasri[2]**

[1]*Dr YSR ANU College of Engineering and Technology, Acharya Nagarjuna University, Guntur -522510, Andhra Pradesh, India*
[2]*Department of Electrical & Electronics Engineering, R.V.R. & J.C. College of Engineering, Guntur - 522 019, Andhra Pradesh, India*
* Corresponding author's Email: anjumahi.2022@gmail.com

Abstract: In today's electrical distribution systems (EDS), the rise of renewable energy sources (RESs) and electric vehicles (EVs) holds immense significance. Despite their positive environmental impact, these technologies pose challenges due to their unpredictable nature. Efficiency and reliability are top priorities for EDSs, which can be achieved through optimal network reconfiguration (ONR). This approach addresses integrating varying RESs and EVs levels by considering distribution losses and the line loadability index (LLI). To enhance network performance by identifying optimal branches and tie-lines for switching, a novel meta-heuristic algorithm, the northern goshawk optimization algorithm (NGO), is proposed. To boost its search capabilities, an improved version, called improved NGO (INGO), introduces a levy flight distribution and an adaptive parameter. Simulations on unified Egyptian network (UEN) system across diverse scenarios demonstrate INGO's computational efficiency surpassing basic NGO and other algorithms like stochastic fractal search (SFS), harmony search algorithm (HAS), and artificial rabbits algorithm (ARO). INGO outperforms in target function optimization and computation time, showcasing its adaptability for real-time applications through reduced losses and enhanced loadability. In the initial network configuration, real power losses were measured at 805.73 kW and reactive power losses at 361.18 kVAr. Notably, the lowest voltage magnitude was recorded at bus-30, reaching 0.9463 p.u. The reliability index SAIDI was calculated as 3.148, corresponding to a maximum loadability of 1.73101 p.u. Following optimal reconfiguration with INGO, significant enhancements were observed. Losses reduced notably to 768.37 kW for real power and 360.86 kVAr for reactive power. The lowest voltage at bus-25 increased to 0.9511 p.u. Furthermore, SAIDI improved to 3.001, while loadability increased to 1.73903 p.u. These improvements were consistent even with varying PV and EV load penetrations.

Keywords: Electrical distribution system, Loss reduction, Voltage stability enhancement, Reactive power compensation, War strategy optimization.

1. Introduction

Modern electrical distribution networks (EDS) are experiencing a significant integration of renewable energy sources (RES) like photovoltaic (PV) and wind turbine (WT) systems, along with the growing presence of electric vehicles (EVs). While this integration brings benefits, it also introduces challenges due to the intermittent nature of RESs, impacting grid stability. Implementing energy storage devices such as energy storage systems (ESS) and pumped hydro storage helps stabilize electricity supply. Smart charging methods and vehicle-to-grid (V2G) technology optimize charging schedules and alleviate grid loads. Advanced monitoring and control technologies, like demand-side management (DMS) with advanced metering infrastructure (AMI), offer real-time data on energy generation, consumption, and grid status. These solutions strive to integrate RESs and EVs into distribution systems for a more sustainable future.

Optimal network reconfiguration (ONR) within

EDS emerges as a valuable tool to manage the influx of renewable energy and EVs by optimizing the distribution system's topology. It minimizes power losses, improves voltage profiles, and enhances grid flexibility to accommodate the varying nature of RESs and EV charging demands. Researchers have contributed diverse solution techniques to address the ONR problem.

A combination of particle swarm optimization (PSO) and harmony search (HS) in [1] tackles the ONR challenge within EDSs. Its aim is to minimize power loss and enhance voltage profiles while adhering to operational and technological constraints. Another approach in [2] utilizes a guided initialization technique to streamline the search space, reducing computational time and improving consistency in finding optimal solutions. This enhancement to the meta-heuristic algorithm aims to minimize power loss and enhance EDS voltage profiles. In [3], a modification to the sigmoid function of selective binary particle swarm optimization (SBPSO) optimizes distribution network configurations, focusing on controlling particle rate of change, exploring search space, and achieving population convergence to reduce power losses. The runner root algorithm (RRA) introduced in [4], inspired by plant runners and roots, effectively tackles ONR problems across two systems. Similarly, [5] explores the use of PSO, genetic algorithm (GA), and exhaustive search (ES) in optimizing power distribution networks. This study evaluates the efficacy of various strategies in solving the ONR problem while minimizing power loss. In [6], optimization of distribution network topologies utilized efficient initial formation, leveraging the bus injection-branch current (BIBC) matrix alongside genetic algorithm (GA) modifications. Meanwhile, [7] focused on enhancing radial unbalanced distribution networks, targeting reduced power losses, improved voltage profiles, and heightened voltage stability index (VSI). The method integrated harmony search (HS) to determine optimal positions for EDS distribution generation (DG) units. Exploring the optimization of EDS topology, [8] employed binary particle swarm optimization (BPSO) and an artificial neural network (ANN) to estimate PV generation and energy storage system (ESS) performance, achieving reduced power losses. This strategy specifically optimized the operation of PV-based DG ESS. Ref [9] introduced a comprehensive approach for enhancing EDS operations by employing deep reinforcement learning (DRL)-assisted multi-objective bacterial foraging optimization (MBFO). This method concurrently optimized objectives including PV power curtailment, voltage variation, power loss, line loading, and generator cost, addressing the non-convex, nonlinear, and multi-objective nature of the optimization problem. In [10], a novel technique is proposed targeting the minimization of real power losses, offering a new approach to tackle the ONR problem for loss reduction in EDS. Addressing the ONR challenge, a selective firefly algorithm (SFA) coupled with load flow analysis criteria was employed to streamline the search space. Additionally, [11] introduced a stochastic fractal search (SFS) technique targeting ONR problem resolution amidst distributed generation (DG), specifically aimed at loss reduction. In [12], a proposal for optimal distribution network reconfiguration and seamless DG integration prioritized maximum DG penetration, voltage profile enhancement, and loss reduction. The model comprehensively considers switching action costs, losses, and DG reactive power generation, simultaneously addressing DG siting, sizing, and operational aspects alongside distribution network reconfiguration (DNR). In [13], modified manta ray foraging optimization algorithm (MRFOA) is introduced for effective control and operation of fully automated distribution networks. This method minimizes power losses while meeting equality and inequality requirements within the Taiwan Power Company (TPC) distribution system. Presenting an innovative approach, [14] utilizes an improved shuffled frog leaping algorithm (ISFLA) to solve ONR, DG sizing, and placement. Its primary aim is to reduce power loss while adhering to operational restrictions. In [15], the study outlines an optimization strategy tackling ONR and DG allocation problems through a modified sequential switch opening and exchange (MSSOE) approach. Its primary contribution is to improve the efficiency and reliability of smart-grid power distribution systems.

“A dynamic and multi-objective distribution network reconfiguration was introduced in [16], featuring a hybrid optimization technique incorporating a performance-boosting loop matrix (LM). This method utilizes the exchange market algorithm (EMA) and wild goat algorithm (WGA) alongside adjustable population size and parallel processing to enhance convergence speed and accuracy. In [17], the improved tunicate swarm intelligent algorithm (ITSA) is presented to address simultaneous ONR, capacitor banks (CBs), and DGs allocation and control. Key objectives encompass reducing energy loss, enhancing voltage profiles, and achieving load balancing. Meanwhile, [18] proposes a novel approach using the ant lion optimizer (ALO) for ONR and DG allocation, aiming to minimize network losses and enhance power quality indices. Simulations conducted on an imbalanced IEEE 33-bus grid, with and without DGs and CBs, demonstrated significant improvements. Introducing an efficient mathematical model for distribution system reconfiguration in [19], the approach minimizes power losses by formulating the problem as a mixed-integer nonlinear programming (MINLP) and solving it through a mathematical programming language (AMPL) solver. Additionally, it offers a comprehensive literature survey and comparison study of various ONR approaches in diverse EDSs.

The aforementioned works show that the ONR problem is heavily addressed to improve various techno-economic benefits in EDS. However, reliability has emerged as a new study dimension for modern EDSs, considering load changes and uncertainties in RESs and EVs, and has been addressed in some recent studies on the ONR problem. In [20], a new strategy proposed to increase the reliability of EDS in the presence of DGs. The deep reinforcement learning (DRL) approach determines the best switches to adjust the power flow, resulting in less loss and greater reliability. A meta-heuristic moth-flame algorithm (MMFA) for ONR and placement of PV and WT based DGs while reducing power losses, improving the voltage profile and stability, and increasing dependability is shown in [21].

Despite the emphasis in the literature on multiple techno, economic, environmental and reliable objectives when tackling ONR and DG allocation challenges, security margin enhancement in light of the emerging high EV load penetration has not been addressed considerably. In this regard, the following key contributions set this study apart from the literature.

1) A multi-objective optimization focusing on technical, reliable and security aspects in solving ONR problem considering RESs and EVs penetration.
2) Improved variant of northern goshawk optimization (INGO) by enhancing search capabilities using Levy Flight distribution and a new adaptive parameter.
3) Simulations are performed on a real-time 30-bus East Delta Network (EDN) of Unified Egyptian Network (UEN) for different scenarios.
4) The computational features of INGO are quantified and compared with basic NGO and stochastic fractal search (SFS), harmony search algorithm (HAS), and artificial rabbits algorithm (ARO).
5) For different scenarios, simulations are performed and highlighted the superiority of INGO and applicability of proposed method for real-time applications.

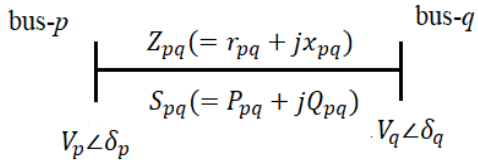

Figure. 1 A simple two-bus distribution network

Additionally, the document is structured as follows. The methodology for evaluating network maximum loadability using the line loadability index is described in section 2. The suggested multi-objective functions and their restrictions are presented in section 3. The mathematical modelling of the suggested INGO and its implementation are provided in section 4. The simulation results and validation are presented in section 5. Finally, section 6 concludes the study.

2. Development of line loadability index

The line loadability index (L_{LI}) [22] is formulated considering a single branch between buses p and q, as shown in Fig. 1. It has an impedance of $Z_{pq}(=r_{pq}+jx_{pq})$ and power flow of $S_{pq}(=P_{pq}+jQ_{pq})$, respectively. The voltage magnitudes for bus-p and bus-q are represented as $V_p\angle\delta_p$ and $V_q\angle\delta_q$, respectively.

The power at receiving bus-q can be determined by:

$$P_{pq}+jQ_{pq} = V_q\angle\delta_q\left(\frac{V_p\angle\delta_p-V_q\angle\delta_q}{r_{pq}+jx_{pq}}\right)^* \quad (1)$$

By separating real and imaginary parts of Eq. (1), the resultants are given by:

$$r_{pq}P_{pq}+x_{pq}Q_{pq} = -V_q^2 + V_p\,V_q cos(\delta_{qp}) \quad (2)$$

$$r_{pq}Q_{pq}-x_{pq}P_{pq} = V_p\,V_q sin(\delta_{qp}) \quad (3)$$

By squaring both sides of Eqs. (2) and (3) and summing, the resultant is given by:

$$V_q^4+2\left(r_{pq}P_{pq}+x_{pq}Q_{pq}-\frac{V_p^2}{2}\right)V_q^2+\left(r_{pq}^2+x_{pq}^2\right)\left(P_{pq}^2+Q_{pq}^2\right)=0 \quad (4)$$

By considering the parameters given in Eq. (5), the Eq. (4) can be reformulated as Eq. (6).

$$\left.\begin{aligned} x &= V_q^2 \;\;\&\;\; a = 1 \\ b &= 2\left(r_{pq}P_{pq} + x_{pq}Q_{pq} - \frac{V_p^2}{2}\right) \\ c &= \left(r_{pq}^2 + x_{pq}^2\right)\left(P_{pq}^2 + Q_{pq}^2\right) \end{aligned}\right\} \tag{5}$$

$$ax^2 + bx + c = 0 \tag{6}$$

The possible solutions for the newly formulated quadratic Eq. (6) can be realised only when its discriminant i.e., $(b^2 - 4ac)$ is greater than or zero and is given by:

$$\frac{V_q^2}{2} - \left(r_{pq}P_{pq} + x_{pq}Q_{pq} - \frac{V_p^2}{2}\right) + \sqrt{\left(r_{pq}^2 + x_{pq}^2\right)\left(P_{pq}^2 + Q_{pq}^2\right)} \geq 0 \tag{7}$$

If $P_{pq} + jQ_{pq}$ is increased to become left term of the Eq. (7) to become zero, then the possible two solutions can become equal that means, the loading point reached to critical loading point or nose point of the PV curve. By replacing $P_{pq} + jQ_{pq}$ as $L_{LI(pq)}\left(P_{pq} + jQ_{pq}\right)$, and then Eq. (7) made equals to zero, the resultant is:

$$L_{LI(pq)} = \frac{V_q^2}{2\left[\left(r_{pq}P_{pq} + x_{pq}Q_{pq} - \frac{V_p^2}{2}\right) + \sqrt{\left(r_{pq}^2 + x_{pq}^2\right)\left(P_{pq}^2 + Q_{pq}^2\right)}\right]} \geq 1 \tag{8}$$

The index $L_{LI(pq)}$ varies from ∞ (i.e., no loading) to 1 (i.e., critically loading). The maximum loading level of a branch can be evaluated by:

$$L_{LI(pq)}\left(P_{pq} + jQ_{pq}\right) \tag{9}$$

For generalizing for this loadability index for a network considering total branches of nbr, then, overall loadability of the network is given by:

$$L_{\overline{LI}} = min\left\{L_{LI(pq)}\left(P_{pq} + jQ_{pq}\right),\ \forall pq = nbr\right\} \tag{10}$$

By finding the minimum of $L_{LI(pq)}$ among all branches, the overall loadability index can be determined as defined in Eq. (10), consequently, by multiplying its basic power flow the maximum loadability (ML) can be evaluated and is given by:

$$ML = L_{\overline{LI}}\left(P_{\overline{pq}} + jQ_{\overline{pq}}\right) \tag{11}$$

where $\overline{pq}$ denotes the branch which has lowest loadability index $L_{\overline{LI}}$ among all branches in the network.

3. Problem formulation

The multi-objective function in this work is formulated to minimize distribution losses, reliability index i.e., system average interruption frequency index (SAIFI) and to maximize network loadability. Mathematically, it is given by.

$$F = P_{loss} + SAIFI + \frac{1}{ML} \tag{12}$$

The above multi-objective function constrained by the following aspects:

$$V_{i,min} \leq V_i \leq V_{i,max};\ i \in nbus \tag{13}$$

$$\overline{nbr} + \overline{ntl} = (nbus - 1) \tag{14}$$

where $nbus$, ntl and nbr are the total number of buses, tie-lines, and branches in the network, respectively; $\overline{nbr}$ and $\overline{ntl}$ are the number of branches and tie-lines which are 'ON' while formulating a new configuration, respectively; $V_{i,min}$ and $V_{i,max}$ are the minimum and maximum limits for voltage magnitudes of bus-*i*, respectively; V_i and P_{loss} are the bus voltage magnitudes and distribution real power loss, which can be evaluated by performing the NR load flow [23].

4. Solution methodology

In this section, the proposed solution methodology using northern goshawk optimization (NGO) [24] and its improvement variant is discussed.

4.1 Northern goshawk optimization

This section describes the process for the suggested solution using an effective and straightforward optimisation technique known as NGO, which was motivated by the hunting habits of the northern goshawk (NG), which is typically found in Eurasia and North America. The NG locates its prey, moves quickly in its direction, and then engages in a brief tail chase. The two phases comprise NG's pursuit of its prey: a swift approach and a quick tail-chase. Before hunting, NGs ponder carefully, and this trait serves as an inspiration for the development of the NGO algorithm. NGO is mathematically described in this section.

The suggested NGO has initialisation,

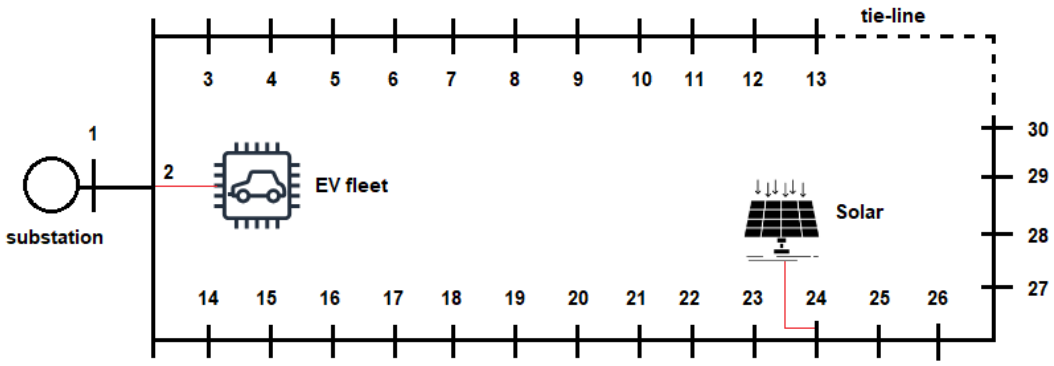

Figure. 2 Schematic diagram of EDN of UEN with assumed PV system and EV fleets

exploration, exploitation as well as termination phases, which are similar to those of any metaheuristic algorithm.

4.1.1. Initialization

At the beginning of the operation, a random initialisation of the population members is performed in the search space. Eqs. (15) and (16), which are used in the proposed NGO algorithm, calculate the population matrix.

$$N = [N_1, N_2, \dots, N_i]^T_{p\times q} \tag{15}$$

$$N_n = [n_1, n_2, \dots, n_i]^T_{q\times 1} \tag{16}$$

where N is the initial population of NGs, N_n is the nth solution, $n_{m\times n}$ is the mth variable value by nth solution vector, p and q are the number of population and search variables, respectively.

Each person is a potential solution, as mentioned previously. Consequently, the attributes of each population member can assess the objective function of the issue. These values are the vectors in Eq. (17) yields.

$$F(N) = \left[F_1 = f_1(n_1), \dots, F_n = f_n(n_n), \dots, F_j = f_j(n_j)\right]^T_{j\times 1} \tag{17}$$

where F is the vector of achieved objective function values and F_n is the fitness value obtained by nth suggested solution.

An ideal solution was selected based on the fitness function value. When limiting or maximising, the proposed solution is more effective. The fitness function values vary in each iteration therefore, the optimal solution should be updated.

4.1.2. Exploration

In this initial stage of exploration, the recognition of the prey and the attack by the NG were modelled. An NG will randomly choose a target prey and attack it immediately. The NGO's exploration capacity is increased in this phase because it can choose random prey from the search area. The search space was exhaustively explored to identify the ideal area. Eqs. (18)–(20) are used to mathematically model the first-step concepts.

$$P_n = N_n,\ n = 1\!:\!p,\ k = 1\!:\!p \tag{18}$$

$$N_{n,m(n,P1)} = \begin{cases} n_{n.m} + r\left(p_{m,n} - In_{n,m}\right) & F_{Pn} < F_n \\ n_{n.m} + r\left(In_{n,m} - p_{m,n}\right) & F_{Pn} \geq F_n \end{cases} \tag{19}$$

$$N_n = \begin{cases} N_{n(n,P1)} & F_{n(n,P1)} < F_n \\ N_n & F_{n(n,P1)} \geq F_n \end{cases} \tag{20}$$

where P_n is the prey position for the nth NG, F_{Pn} is the fitness value, k is the real number between 1 and q, r is a uniformly distributed random number between 0 and 1, $N_{n(n,P1)}$ is the new position for the nth solution, $N_{n(n,P1)}$ is the fitness of new position, $N_{n,m(n,P1)}$ is its m th position, $F_{n(n,P1)}$ is the fitness value at the first phase or exploration phase, I is a random number that can be either 1 and 2.

4.1.3. Exploitation

After the NG attacks, the prey ran away. The northern goshawk continued to pursue its prey. The quickness of the NGs allows them to hunt in practically anyplace. This method can perform in-depth local searches of the search space by simulating this behaviour. The NGO algorithm advises scouting a target area with a radius of R. Eqs. (21)–(23) are used to mathematically model the notions of the second phase.

$$N_{n,m(n,P2)} = n_{n,m} + R(2r - 1)n_{n,m} \tag{21}$$

Received: December 28, 2023. Revised: January 26, 2024.

Table 1. Comparison of different case studies in Scenario-1

Case	Branches		P_{loss} (kW)	Q_{loss} (kVAr)	V_{min} (p.u.)	SAIF1	$L_{\overline{LI}}$
	Open	Close					
Base [27]	30	1 to 29	805.73	361.18	0.9463 (30)	3.148	1.73101
ONR by INGO	24	1 to 23 & 25 to 30	768.37	360.86	0.9511 (25)	3.001	1.73903

Table 2. Comparison of different algorithms for ONR problem in Scenario-1

Algorithm	Branches		Worst	Best	Mean	Median	S.D.	Time (min)
	Open	Close						
SFS [28]	24	1 to 23 & 25 to 30	932.422	768.370	778.220	768.370	30.366	3.546
HAS [29]	24	1 to 23 & 25 to 30	895.614	768.370	774.176	768.370	25.355	3.136
ARO [30]	24	1 to 23 & 25 to 30	879.220	768.370	791.848	808.977	23.914	3.286
NGO [24]	24	1 to 23 & 25 to 30	880.180	768.370	771.462	768.370	16.699	3.327
INGO [25]	24	1 to 23 & 25 to 30	883.541	768.370	770.767	768.370	16.281	3.122

Table 3. Comparison of different case studies in Scenario-2

Case	Branches		P_{loss} (kW)	Q_{loss} (kVAr)	V_{min} (p.u.)	SAIF1	$L_{\overline{LI}}$
	Open	Close					
Case 1 (base)	30	1 to 29	723.85	326.88	0.9514 (30)	3.1476	1.7982
Case 1 (ONR)	25	1 to 24 & 26 to 30	698.46	323.92	0.9582 (26)	2.9800	1.7998
Case 2 (base)	30	1 to 29	848.15	384.75	0.9454 (30)	3.1476	1.6431
Case 2 (ONR)	24	1 to 23 & 25 to 30	810.66	384.39	0.9502 (25)	3.0014	1.6449
Case 3 (base)	30	1 to 29	764.528	349.496	0.9505 (30)	3.1476	1.6979
Case 3 (ONR)	25	1 to 24 & 26 to 30	739.048	346.506	0.9573 (26)	2.9803	1.6993

$$R = 0.02\left(1 - \frac{t}{T_{max}}\right) \quad (22)$$

$$N_n = \begin{cases} N_{n(n,P2)} & F_{n(n,P2)} < F_n \\ N_n & F_{n(n,P2)} \geq F_n \end{cases} \quad (23)$$

where t and T_{max} are the current and maximum iteration number, respectively; $N_{n(n,P2)}$ is the new position for the kth solution, $F_{n(n,P2)}$ is the fitness of new position, $N_{n,m(n,P2)}$ is its mth position, $F_{n(n,P2)}$ is the fitness value at the second phase or exploration phase.

An iteration is completed after updating every member of the population using the first and second stages of the proposed NGO algorithm. At this stage, the ideal solution, fitness value, and new population size are chosen. Then, the algorithm keeps updating the population members based on Eqs. (18)–(23) until the end of the program. The best suggested solution from the algorithm iterations is offered as a quasi-optimal solution for the optimisation problem once the NGO technique is fully applied.

4.2 Improved northern goshawk optimization

The basic NGO is stuck in a local minimum. This frequently occurs in complex high-dimensional optimisation problems. Levy flight (LF) is added to the NGO algorithm to boost the search capabilities for difficult real-world issues. LF has improved resource search efficiency hence they have been included in the INGO [25]. The second portion of Eqs. (19), (21), and (22) are updated by:

$$N_{n,m(n,P1)} = n_{n.m} + LF\left(In_{n,m} - p_{m,n}\right) \quad F_{Pn} \geq F_n \quad (24)$$

$$N_{n,m(n,P2)} = n_{n,m} + \alpha\beta(2r-1)n_{n,m} + K \quad (25)$$

where LF is Levy Flight distribution [26]. The exploitation parameter α can be set to 0.0001. The adaptive parameter β is added to the smooth transition from exploration to exploitation, can be computed as follows:

$$K = \beta \times I \quad (26)$$

$$\beta = 1.99\left(0.99 - \frac{t}{T_{max}}\right) \quad (27)$$

By having these modifications, the performance of basic NGO is improved significantly in comparison with various other meta-heuristics as proved in [25].

5. Results and discussion

Simulations are performed on a real-time 30-bus east delta network (EDN) of unified Egyptian network (UEN) [27] for different scenarios using programming in MATLABR2023a. The PC has 16 GB RAM and Intel Core i3 Processor.

Two scenarios are simulated. In Scenario, ONR problem is solved using basic NGO [24] and stochastic fractal search (SFS) [28], harmony search algorithm (HAS) [29], and artificial rabbits algorithm (ARO) [30] and compared with INGO [25]. In Scenario-2, three case studies are compared considering: (a) only RESs penetration, (b) only EVs penetration and (c) both RESs and EVs penetration.

5.1 Comparative study

The standard east delta network (EDN) of unified Egyptian network (UEN) data is taken from [27]. The modified system by considering solar photovoltaic (SPV) system of 1 MW at bus-24 and EV fleet of 1.5 MW at bus-2 is shown in Fig. 2. The tie-line data which is not provided in [27] is assumed as (0.5 + *j* 1.0) ohm.

The standard EDN of UEN has total real and reactive power loads of 22441.3 kW and 14162.2 kVAr, respectively. The network is operating at 11 kV. The Newton Raphson (NR) load flow [23] is used to compute bus voltage profile and branch power flows as well as total distribution losses.

For the radial configuration, without considering tie-line, the system has total of real and reactive power losses of 805.73 kW and 361.18 kVAr, respectively [27]. The network has lowest voltage magnitude of 0.9463 p.u. is observed at bus-29 and 30. Further, the SAIFI and $L_{\overline{LI}}$ are determined as 3.148 and 1.73101, respectively.

For ONR, the tie-line 30 is closed and INGO is used to identify the branch which is to be opened for formulating again best configuration. As per the results of INGO, the optimal branch for opening is 24 and correspondingly, the network performance is evaluated and given in Table 1. The total real and reactive power losses are of 805.73 kW and 361.18 kVAr, respectively. The network lowest voltage magnitude at bus-25 is raised to 0.9511 p.u. Further, the SAIFI is decreased to 3.001 and $L_{\overline{LI}}$ is raised to and 1.73903. These figures are clearly indicating that the performance of system is improved significantly by reducing losses, improving reliability and enhancing loadability index.

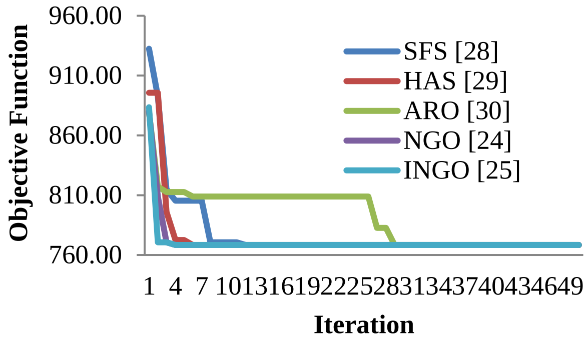

Figure. 3 Convergence of compared algorithms

The performance of INGO is further compared with other meta-heuristics namely SFS [28], HAS [29], ARO [30] and basic NGO [24]. The case study is repeated for 25 independent runs and the results are quantified with statistical measures and given in Table 2. As per the low standard deviation (S.D), mean, median and computational times, INGO is outperformed other algorithms, though the best result is same. This indicates the enhancement in search characteristics of basic NGO with the proposed modifications as described in Section 4.2. The convergence characteristics of all the algorithms for best results are given in Fig. 3.

5.2 Simulations on modified system

In the modified system, SPV and EV fleets are considered. The simulations in this scenario are performed only using INGO and the results are compared for all cases in Table 3.

5.2.1. Case 1 (only SPV penetration)

By having 1 MW SPV system at bus-24, the results are discussed for base case (i.e., original radial configuration) and optimal configuration. The total real and reactive power losses are determined as 723.85 kW and 326.88 kVAr, respectively. The system has lowest voltage magnitude at bus-30 as 0.9514 p.u. Further, there is no change in SAIFI due to same configuration, however, $L_{\overline{LI}}$ is raised to 1.7982 due to the presence of SPV in the network.

As per the results of INGO, the optimal branch for opening is 25 and correspondingly, the network performance is evaluated. The total real and reactive power losses are reduced to 698.46 kW and 323.92 kVAr, respectively. The network lowest voltage magnitude at bus-26 is raised to 0.9582 p.u. Further, the SAIFI is decreased to 2.980 and $L_{\overline{LI}}$ is raised considerably to 1.7998.

5.2.2. Case 2 (only EV fleet penetration)

By having 1.5 MW EV fleet at bus-2, the results are discussed for base case (i.e., original radial configuration) and optimal configuration. The operating power factor of EV fleet is treated as 0.85 lagging. Thus, the total network load is raised to 23941.3 kW and 14655.23 kVAr, respectively. Consequently, the total real and reactive power losses are registered as 848.15 kW and 384.75 kVAr, respectively. The system has lowest voltage magnitude at bus-30 as 0.9454 p.u. Further, there is no change in SAIFI due to same configuration, however, $L_{\overline{LI}}$ is decreased to 1.6431 due to the presence of EV fleet load in the network.

As per the results of INGO, the optimal branch for opening is 24 and correspondingly, the network performance is evaluated. The total real and reactive power losses are reduced to 810.66 kW and 384.39 kVAr, respectively. The network lowest voltage magnitude at bus-24 is raised to 0.9502 p.u. Further, the SAIFI is decreased to 3.0014 and $L_{\overline{LI}}$ is raised considerably to 1.6449. In comparison to base case, ONR resulted for improvement in performance.

5.2.3. Case 3 (both SPV and EV fleet penetration)

In this case, by having both SPV and EF fleet, the results are discussed for base case (i.e., original radial configuration) and optimal configuration. The total real and reactive power losses are registered as 764.528 kW and 349.496 kVAr, respectively. The system has lowest voltage magnitude at bus-30 as 0.9505 p.u. Further, there is no change in SAIFI due to same configuration, however, $L_{\overline{LI}}$ is decreased to 1.6979 due to the presence of EV fleet load in the network.

As per the results of INGO, the optimal branch for opening is 24 and correspondingly, the network performance is evaluated. The total real and reactive power losses are reduced to 739.048 kW and 346.506 kVAr, respectively. The network lowest voltage magnitude at bus-26 is raised to 0.9573 p.u. Further, the SAIFI is decreased to 2.9803 and $L_{\overline{LI}}$ is raised considerably to 1.6993. In comparison to base case, ONR resulted for improvement in performance.

While INGO has demonstrated its effectiveness, there remains a need to assess its performance in comparison to emerging state-of-the-art metaheuristics. These include the four directed search algorithm (FDSA) [31], walk-spread algorithm (WSA) [32], attack leave optimizer (ALO) [33], total interaction algorithm (TIA) [34], and migration-crossover algorithm (MCA) [35]. This serves as an extension of our ongoing research work. Additionally, numerous IEEE standard test systems like IEEE 33-, 69-, 85-, and 118-bus EDNs have been extensively referenced in literature. Extending this research involves applying the proposed methods to these systems and conducting a comparative analysis to establish benchmarks.

6. Conclusion

To manage RESs and EV fleet loads in EDSs, this paper proposes a multi-objective optimisation that focuses on technical, reliable, and security aspects when solving the ONR problem based on the penetration of RESs and EVs. To solve the optimisation problem, a variant of northern goshawk optimisation (INGO) with enhanced search capabilities using the Levy Flight distribution and a new adaptive parameter was presented. Different scenarios were simulated on a 30-bus real-time east delta network (EDN) of the unified Egyptian network (UEN). INGO's computational characteristics are quantified and compared with those of NGO, SFS, HAS, and ARO. Simulations were performed for various scenarios, demonstrating the superiority of INGO and viability of the proposed method for real-time applications. The initial network exhibited 805.73 kW real and 361.18 kVAr reactive power losses, with the lowest voltage at bus-30 (0.9463 p.u.). Post INGO reconfiguration, losses dropped to 768.37 kW and 360.86 kVAr, raising bus-25's voltage to 0.9511 p.u. SAIDI improved to 3.001, with increased loadability at 1.73903 p.u.

Conflicts of interest

The authors declare no conflict of interest.

Author contributions

Conceptualization, methodology, software and original draft preparation are done by Lalitha Kondisetti; supervision, review, and formal analysis are done by Katragadda Swarnasri.

Notations list

Z_{pq}	Impedance of branch *p-q*
r_{pq}	Resistance of branch *p-q*
x_{pq}	Reactance of branch *p-q*
S_{pq}	Complex power flow through branch *p-q*
P_{pq}	Real power flow through branch *p-q*
Q_{pq}	Reactive power flow through branch *p-q*
$L_{LI(pq)}$	Loadability index of branch *p-q*
$L_{\overline{LI}}$	Overall loadability index of network
ML	Maximum loadability
V_p & V_q	Voltage magnitudes of buses *p* and *q*
δ_p & δ_q	Load angles of buses *p* and *q*

$nbus$	Number of buses
ntl	Number of tie-lines
nbr	Number of branches
$\overline{nbr}$	Number of branches in reconfiguration
$\overline{ntl}$	Number of tie-lines in reconfiguration
$V_{i,min}$	Minimum limit for voltage magnitude
$V_{i,max}$	Maximum limit for voltage magnitude
P_{loss}	Real power loss

References

[1] A. O. Salau, Y. W. Gebru, and D. Bitew, "Optimal network reconfiguration for power loss minimization and voltage profile enhancement in distribution systems", *Heliyon*, Vol. 6, No. 6, 2020.

[2] M. A. Samman, H. Mokhlis, N. N. Mansor, H. Mohamad, H. Suyono, and N. M. Sapari, "Fast optimal network reconfiguration with guided initialization based on a simplified network approach", *IEEE Access*, Vol. 8, pp. 11948-11963, 2020.

[3] R. Pegado, Z. Ñaupari, Y. Molina, and C. Castillo, "Radial distribution network reconfiguration for power losses reduction based on improved selective BPSO", *Electric Power Systems Research*, Vol. 169, pp. 206-213, 2019.

[4] T. T. Nguyen, "Electric distribution network reconfiguration for power loss reduction based on runner root algorithm", *International Journal of Electrical and Computer Engineering (IJECE)*, Vol. 10, No. 5, pp. 5016-5024, 2020.

[5] O. Kahouli, H. Alsaif, Y. Bouteraa, N. B. Ali, and M. Chaabene, "Power system reconfiguration in distribution network for improving reliability using genetic algorithm and particle swarm optimization", *Applied Sciences*, Vol. 11, No. 7, p. 3092, 2021.

[6] D. Jakus, R. Čađenović, J. Vasilj, and P. Sarajčev, "Optimal reconfiguration of distribution networks using hybrid heuristic-genetic algorithm", *Energies*, Vol. 13, No. 7, p. 1544, 2020.

[7] A. Roosta, H. R. Eskandari, and M. H. Khooban, "Optimization of radial unbalanced distribution networks in the presence of distribution generation units by network reconfiguration using harmony search algorithm", *Neural Computing and Applications*, pp. 7095-7109, 2019.

[8] R. V. Monteiro, J. P. Bonaldo, R. F. D. Silva, and A. S. Bretas, "Electric distribution network reconfiguration optimized for PV distributed generation and energy storage", *Electric Power Systems Research*, Vol. 184, p. 106319, 2020.

[9] Y. Li, G. Hao, Y. Liu, Y. Yu, Z. Ni, and Y. Zhao, "Many-objective distribution network reconfiguration via deep reinforcement learning assisted optimization algorithm", *IEEE Transactions on Power Delivery*, Vol. 37, No. 3, pp. 2230-2244, 2021.

[10] C. Gerez, L. I. Silva, E. A. Belati, A. J. S. Filho, and E. C. Costa, "Distribution network reconfiguration using selective firefly algorithm and a load flow analysis criterion for reducing the search space", *IEEE Access*, Vol. 7, pp. 67874-67888, 2019.

[11] T. T. Tran, K. H. Truong, and D. N. Vo, "Stochastic fractal search algorithm for reconfiguration of distribution networks with distributed generations", *Ain Shams Engineering Journal*, Vol. 11, No. 2, pp. 389-407, 2020.

[12] A. Bagheri, M. Bagheri, and A. Lorestani, "Optimal reconfiguration and DG integration in distribution networks considering switching actions costs using tabu search algorithm", *Journal of Ambient Intelligence and Humanized Computing*, pp. 7837-7856, 2021.

[13] E. E. Elattar, A. M. Shaheen, A. M. E. Sayed, R. A. E. Sehiemy, and A. R. Ginidi, "Optimal operation of automated distribution networks based-MRFO algorithm", *IEEE Access*, Vol. 9, pp. 19586-19601, 2021.

[14] J. Siahbalaee, N. Rezanejad, and G. B. Gharehpetian, "Reconfiguration and DG sizing and placement using improved shuffled frog leaping algorithm", *Electric Power Components and Systems*, Vol. 47, No. 16-17, pp. 1475-1488, 2019.

[15] V. Vai, S. Suk, R. Lorm, C. Chhlonh, S. Eng, and L. Bun, "Optimal reconfiguration in distribution systems with distributed generations based on modified sequential switch opening and exchange", *Applied Sciences*, Vol. 11, No. 5, p. 2146, 2021.

[16] A. Jafari, H. G. Ganjehlou, F. B. Darbandi, B. M. Ivatloo, and M. Abapour, "Dynamic and multi-objective reconfiguration of distribution network using a novel hybrid algorithm with parallel processing capability", *Applied Soft Computing*, Vol. 90, p. 106146, 2020.

[17] T. Fetouh and A. M. Elsayed, "Optimal control and operation of fully automated distribution networks using improved tunicate swarm intelligent algorithm", *IEEE Access*, Vol. 8, pp. 129689-129708, 2020.

[18] M. J. Moghaddam, A. Kalam, J. Shi, S. A.

Nowdeh, F. H. Gandoman, and A. Ahmadi, "A new model for reconfiguration and distributed generation allocation in distribution network considering power quality indices and network losses", *IEEE Systems Journal*, Vol. 14, No. 3, pp. 3530-3538, 2020.

[19] M. Mahdavi, H. H. Alhelou, N. D. Hatziargyriou, and A. A. Hinai, "An efficient mathematical model for distribution system reconfiguration using AMPL", *IEEE Access*, Vol. 9, pp. 79961-79993, 2021.

[20] S. Malekshah, A. Rasouli, Y. Malekshah, A. Ramezani, and A. Malekshah, "Reliability-driven distribution power network dynamic reconfiguration in presence of distributed generation by the deep reinforcement learning method", *Alexandria Engineering Journal*, Vol. 61, No. 8, pp. 6541-6556, 2022.

[21] A. J. Nowdeh, M. Babanezhad, S. A. Nowdeh, A. Naderipour, H. Kamyab, Z. A. Malek, and V. K. Ramachandaramurthy, "Meta-heuristic matrix moth–flame algorithm for optimal reconfiguration of distribution networks and placement of solar and wind renewable sources considering reliability", *Environmental Technology & Innovation*, Vol. 20, p. 101118, 2020.

[22] J. Yu, W. Li, and W. Yan, "A new line loadability index for radial distribution systems", *Electric Power Components and Systems*, Vol. 36, No. 11, pp. 1245-1252, 2008.

[23] R. D. Zimmerman, C. E. M. Sánchez, and R. J. Thomas, "MATPOWER: Steady-state operations, planning, and analysis tools for power systems research and education", *IEEE Transactions on Power Systems*, Vol. 26, No. 1, pp. 12-19, 2010.

[24] M. Dehghani, Š. Hubálovský, and P. Trojovský, "Northern goshawk optimization: a new swarm-based algorithm for solving optimization problems", *IEEE Access*, Vol. 9, pp. 162059-162080, 2021.

[25] H. T. Sadeeq and A. M. Abdulazeez, "Improved Northern Goshawk Optimization Algorithm for Global Optimization", In: *Proc. of 2022 4th International Conference on Advanced Science and Engineering (ICOASE)*, pp. 89-94, Sep. 2022, *IEEE*.

[26] E. H. Houssein, M. R. Saad, F. A. Hashim, H. Shaban, and M. Hassaballah, "Lévy flight distribution: A new metaheuristic algorithm for solving engineering optimization problems", *Engineering Applications of Artificial Intelligence*, Vol. 94, p. 103731, 2020.

[27] A. A. A. E. Ela, R. A. E. Sehiemy, A. M. Kinawy, and M. T. Mouwafi, "Optimal capacitor placement in distribution systems for power loss reduction and voltage profile improvement", *IET Generation, Transmission & Distribution*, Vol. 10, No. 5, pp. 1209-1221, 2016.

[28] H. Salimi, "Stochastic fractal search: a powerful metaheuristic algorithm", *Knowledge-Based Systems*, Vol. 75, pp. 1-8, 2015.

[29] X. S. Yang, "Harmony search as a metaheuristic algorithm", *Music-Inspired Harmony Search Algorithm: Theory and Applications*, pp. 1-4, 2009.

[30] L. Wang, Q. Cao, Z. Zhang, S. Mirjalili, and W. Zhao, "Artificial rabbits optimization: A new bio-inspired meta-heuristic algorithm for solving engineering optimization problems", *Engineering Applications of Artificial Intelligence*, Vol. 114, p. 105082, 2022.

[31] P. Kusuma and A. Dinimaharawati, "Four Directed Search Algorithm: A New Optimization Method and Its Hyper Strategy Investigation", *International Journal of Intelligent Engineering and Systems*, Vol. 16, No. 5, pp. 598-611, 2023, doi: 10.22266/ijies2023.1031.51.

[32] P. Kusuma and A. L. Prasasti, "Walk-Spread Algorithm: A Fast and Superior Stochastic Optimization", *International Journal of Intelligent Engineering and Systems*, Vol. 16, No. 5, pp. 275-288, 2023, doi: 10.22266/ijies2023.1031.24.

[33] P. D. Kusuma and F. C. Hasibuan, "Attack Leave Optimizer: A New Metaheuristic that Focuses on The Guided Search and Performs Random Search as Alternative", *International Journal of Intelligent Engineering and Systems*, Vol. 16, No. 3, pp. 244–257, 2023, doi: 10.22266/ijies2023.0630.19.

[34] P. D. Kusuma and A. Novianty, "Total Interaction Algorithm: A Metaheuristic in Which Each Agent Interacts with All Other Agents", *International Journal of Intelligent Engineering and Systems*, Vol. 16, No. 1, pp. 224-234, 2023, doi: 10.22266/ijies2023.0228.20.

[35] P. D. Kusuma and M. Kallista, "Migration-Crossover Algorithm: A Swarm-based Metaheuristic Enriched with Crossover Technique and Unbalanced Neighbourhood Search", *International Journal of Intelligent Engineering and Systems*, Vol. 17, No. 1, pp. 698-710, 2024, doi: 10.22266/ijies2024.0229.59.